

RESEARCH ARTICLE

10.1002/2013JD021352

Key Points:

- The QBO-induced residual circulation is the main cause of the HT effect
- A broader and strengthened polar vortex caused a weaker HT effect in 1978–1997
- Waves ducted meridionally away from the vortex interfered with the HT effect

Correspondence to:

H. Lu,
hlu@bas.ac.uk

Citation:

Lu, H., T. J. Bracegirdle, T. Phillips, A. Bushell, and L. Gray (2014), Mechanisms for the Holton-Tan relationship and its decadal variation, *J. Geophys. Res. Atmos.*, 119, 2811–2830, doi:10.1002/2013JD021352.

Received 12 DEC 2013

Accepted 21 FEB 2014

Accepted article online 24 FEB 2014

Published online 18 MAR 2014

Mechanisms for the Holton-Tan relationship and its decadal variation

Hua Lu¹, Thomas J. Bracegirdle¹, Tony Phillips¹, Andrew Bushell², and Lesley Gray^{3,4}

¹British Antarctic Survey, Cambridge, UK, ²Met Office, Exeter, UK, ³National Centre for Atmospheric Science, UK, ⁴Department of Physics, University of Oxford, Oxford, UK

Abstract This study provides a mechanistic explanation of why the Holton-Tan (HT) effect, a phenomenon in which the strength of northern stratospheric winter polar vortex synchronizes with the equatorial quasi-biennial oscillation (QBO), was disrupted in the middle to late winters of 1978–1997. In line with recent reassessments of the HT effect, we find that an easterly QBO in the lower stratosphere leads to the formation of a midlatitude wave guide that enhances both the upward propagating planetary waves from the troposphere into the lower stratosphere (~35–50°N, 30–200 hPa) and the northward wave propagation in the upper to middle stratosphere (~35–60°N, 20–5 hPa). This enhanced poleward refraction of planetary waves results in a more disturbed polar vortex, causing the HT effect. The weakening of the HT effect in 1978–1997 was associated with a broader and strengthened polar vortex in November to January. The divergence of wave activity generated by eddies growing within the vortex provided the momentum source and allowed wave activity to propagate meridionally away from the vortex; this interfered with the QBO modulation of planetary wave propagation and led to a weakening of the HT effect during this period. The stronger than average polar vortex in 1978–1997 was associated with a vertically coherent cooling signature over northeastern Asia in the stratosphere. We suggest that a change of stratospheric circulation and/or a change of the stratosphere-troposphere coupling were the main causes for the disrupted HT effect in 1978–1997.

1. Introduction

A relationship between the equatorial quasi-biennial oscillation (QBO) and the northern stratospheric winter polar vortex, often referred to as the Holton-Tan effect (HT effect hereafter), has been the subject of studies since the 1980s [Holton and Tan, 1980, 1982] (for more recent reviews, see Baldwin *et al.* [2001] and Anstey and Shepherd [2013]). It is a phenomenon in which the strength of the stratospheric winter polar vortex is influenced by the equatorial quasi-biennial oscillation (QBO). More specifically, the vortex becomes stronger and colder when the QBO is in its westerly phase (wQBO) and weaker and warmer when the QBO is in its easterly phase (eQBO). In the Northern Hemisphere (NH) winter, the HT effect is most apparent for a QBO definition that is based on the equatorial zonal wind or zonal wind anomaly in the lower stratosphere (~50 hPa) [Holton and Tan, 1980; Garfinkel *et al.*, 2012], or equivalently by the equatorial vertical zonal wind shear between 50 hPa and 70 hPa [Hitchman and Huesmann, 2009]. More frequent sudden stratospheric warmings (SSWs) during eQBO give rise to warmer temperatures and weaker zonal mean zonal winds in the polar stratosphere. Observational studies have also found that the HT effect is most significant in early to middle winter and weaker in late winter [Dunkerton and Baldwin, 1991; Naito and Hirota, 1997; Lu *et al.*, 2008]. The HT effect has been successfully reproduced both by simple mechanistic models in which a QBO is forced at the equator [e.g., Gray and Pyle, 1989; O'Sullivan and Salby, 1990; O'Sullivan and Young, 1992; Naito and Yoden, 2006] and by complex general circulation models in which the QBO is either imposed [Balachandran and Rind, 1995; Hamilton, 1998; Garfinkel *et al.*, 2012] or generated internally through a parameterization of gravity waves [Calvo *et al.*, 2009; Marshall and Scaife, 2009; Naoe and Shibata, 2010; Yamashita *et al.*, 2011]. Nevertheless, the underlying mechanism causing the HT effect is still not clearly identified.

Holton and Tan [1980, 1982] were the first to propose a dynamic mechanism for the observed HT effect. They hypothesized that a change of subtropical critical line (i.e., zero wind line) in the lower stratosphere alters the width of the extratropical wave guide for quasi-stationary planetary waves propagating into the stratosphere from the troposphere. Under eQBO, the critical line is shifted toward Northern Hemisphere (NH) subtropics, and this narrows the midlatitude wave guide; the critical line can reflect planetary waves back toward the pole [Tung, 1979; Killworth and McIntyre, 1985], which results in a deceleration of the polar vortex. Conversely, under wQBO, the critical layer is located in the summer hemisphere so that planetary waves are able to propagate more easily

into the tropical latitudes and become less confined to the winter hemisphere, resulting in a less disturbed, colder polar vortex. This mechanism is most well known and is referred as the critical-line mechanism hereafter.

Many studies have found changes of planetary wave amplitude and/or Eliassen-Palm (EP) fluxes and EP flux convergence in relation to the QBO [Holton and Tan, 1982; Holton and Austin, 1991; Dunkerton and Baldwin, 1991; Balachandran and Rind, 1995; Hu and Tung, 2002a; Ruzmaikin et al., 2005; Naito and Yoden, 2006; Yamashita et al., 2011]. However, it remains unclear whether or not the critical-line mechanism is the primary mechanism for these wave changes. In the lower stratosphere, planetary wave anomalies that are weaker than, or even opposite to, what one would expect from the HT mechanism have been reported [Dunkerton and Baldwin, 1991; Ruzmaikin et al., 2005; Naoe and Shibata, 2010; Yamashita et al., 2011]. It is still unclear why the QBO modulation of upward propagating stationary planetary waves changes from early winter to late winter [Holton and Tan, 1982; Hu and Tung, 2002a] and why the QBO-induced wave anomalies differ from one study to another at the same latitude [Ruzmaikin et al., 2005; Naoe and Shibata, 2010]. Watson and Gray [2013] suggested that the influence of the subtropical critical line in reflecting planetary waves may be important but predicting its impact is not as straightforward as previous studies have assumed because of feedback processes that are initiated as a result of the wave forcing.

Apart from the critical-line mechanism, it has also been proposed that the QBO may affect planetary wave propagation via the QBO-induced meridional circulation [Kodera, 1991; Ruzmaikin et al., 2005; Garfinkel et al., 2012]. In particular, Garfinkel et al. [2012] carried out a range of experimental runs using the Whole Atmosphere Community Climate Model by imposing a range of vertical profiles of eQBO at the equator and with fixed radiative forcing for perpetual January or February. By taking composite differences between their forced eQBO runs and their control runs, they found that significant changes of EP fluxes and EP flux divergence occur mainly in the middle to upper stratosphere (~ 5 hPa) rather than in the lower stratosphere, in agreement with earlier studies [Naoe and Shibata, 2010; Yamashita et al., 2011]. Garfinkel et al. [2012] separately examined the critical line in the subtropical lower stratosphere and the QBO-induced meridional circulation in the middle to upper stratosphere in relation to the QBO-modulated EP flux divergences. They found that the latter affects horizontally propagating EP fluxes in the middle stratosphere via a change of wave guide at ~ 35 – 50°N , where anomalously smaller values of the refractive index (n^2) were detected in their eQBO forced runs. The negative n^2 anomalies expand poleward with time and create a barrier to planetary wave propagation from subpolar latitudes into midlatitudes at ~ 5 hPa. This enhances planetary wave convergence in the polar region and therefore causes a weaker polar vortex.

A third possible mechanism is related to the QBO in the equatorial upper stratosphere. Gray et al. [2001] and Gray [2003] found that the winds and/or the vertical wind shear in the equatorial upper stratosphere affect the evolution of the polar vortex and the frequency and timing of major SSWs. These authors suggested that planetary waves of very deep structure span the entire depth of the stratosphere. Subtropical upper stratospheric wind anomalies can modulate the planetary waves and the polar vortex in a similar manner via either a modulation of subtropical critical line or the QBO-induced meridional circulation. As the QBO in the upper stratosphere tends to be in phase with the QBO in the lower stratosphere, the upper level QBO may be responsible for the observed HT effect [Naoe and Shibata, 2010]. Thus, a common feature of all three aforementioned mechanisms is that a QBO modulation of planetary waves is involved.

The polar vortex is sensitive to many factors in both the troposphere and the stratosphere [Garfinkel and Hartmann, 2008]. A combination of concurrent forcings cannot be added linearly because the vortex strength can be dominated by one factor and become less sensitive to others [Holton and Austin, 1991; Camp and Tung, 2007; Calvo et al., 2009]. Studies have shown that tropospheric variability associated with factors such as North Pacific sea surface temperature, El Niño-Southern Oscillation (ENSO), and volcanic eruptions are all able to disrupt the HT effect [Wei et al., 2007; Garfinkel and Hartmann, 2008; Calvo et al., 2009]. Additionally, the 11 year solar cycle can also disrupt the HT effect [Labitzke and van Loon, 1988; Gray et al., 2001; Lu et al., 2009]. The nonlinear interaction among these processes makes it harder to identify the mechanism responsible for the HT effect as well as what may cause its interannual to decadal-scale variations [Anstey and Shepherd, 2013]. It remains largely unknown mechanistically how the other factors interfere with the HT effect.

Here we study one particular variation of the HT effect. Lu et al. [2008] found that the disruptions of the HT effect occurred on two distinctly different decadal time scales; one is by the 11 year solar cycle [Labitzke and van Loon, 1988; Lu et al., 2009] and the other is over 1977–1997, a period spanning nearly two 11 year solar

cycles and hence containing roughly the same number of years of high and low solar activity. The disruption of the HT effect in 1977–1997 started in December and intensified in late winter, during which period the sign of the HT effect even reversed. During solar minimum conditions and in 1959–1976 and 1998–2006, the HT effect remained statistically significant for the extended winter period (October–March). Also, *Lu et al.* [2008] found that the weakening of the HT effect during 1977–1997 was associated with a seasonal shift of the timing of SSWs. While more SSWs occurred under eQBO during early to middle winter pre-1976 and after 1997, more SSWs occurred in wQBO in late winter during 1977–1997. *Anstey and Shepherd* [2008] suggested that the decadal variation of the HT effect may be affected by the seasonal alignment of QBO phase transitions. However, it remains mechanistically unclear why the HT effect is weakened and how the seasonal clustering of the QBO phase transition plays a role in altering the HT effect.

This study has two main objectives: (1) to gain further insight into the dynamical processes that underpin the HT effect and (2) to provide mechanistic understanding of the disrupted HT effect in middle to late winters of 1977–1997. The seasonal progression of the HT effect and its decadal variation are presented in section 3.1. The evidence provided by (i) QBO modulation of EP fluxes and EP flux divergence, (ii) the residual mean meridional circulation, and (iii) quasi-stationary planetary wave guides is given in section 3.2. The process that causes the weakening of the HT effect in 1977–1997 is examined in section 3.3.

2. Data and Methods

We make use of daily and monthly data from the European Centre for Medium-range Weather Forecasts (ECMWF) Re-Analysis (ERA)-Interim data set [*Dee and Uppala*, 2009] for the period 1979–2011 and the ERA-40 data set for the period of 1958–2001 [*Uppala et al.*, 2005] to assess the period spanning January 1958 to December 2011. For both data sets, data archived at $2.5^\circ \times 2.5^\circ$ grid spacing resolution and 23 pressure levels from 1000 hPa to 1 hPa are used. We carried out the same analyses by merging the data sets including either the full length of ERA-40 or ERA-Interim data for the overlapping period (i.e., 1979–2001) and by using the two data sets separately. At the places where the results from the two data sets are similar, we only report the results from the merged data set created by keeping the full length of ERA-Interim data from January 1979 onward and back extending to 1958 using ERA-40. Where the results differ, the difference between the two data sets will be discussed. The benefit of using two data sets is that it allows us to test the robustness of the statistics and therefore better identify the responsible mechanisms.

As in previous studies [i.e., *Holton and Tan*, 1980; *Lu et al.*, 2008], the QBO is estimated from the cosine-weighted averages of zonal mean zonal wind at 5°S – 5°N , 50 hPa, and then deseasonalized based on the climatological mean. We shall show later that at monthly to seasonal time scales, the difference between the QBOs estimated from the two ECMWF data sets is negligibly small. For the composite analysis, the wQBO and eQBO were defined as the $\text{QBO} \geq 2$ and $\leq -2 \text{ m s}^{-1}$, respectively.

We examine a range of diagnostics including EP fluxes and EP flux divergence, the quasi-geostrophic refractive index, and the mean meridional circulation. More specifically, we study QBO modulation of wave-mean flow interaction and its decadal variation in terms of two properties: (1) the strength and direction of planetary wave propagation, convergence, and divergence; and (2) the anomalous wave guide formation. We use the transformed Eulerian-mean (TEM) equation to study the first property and the refractive index for the second property. Both methods and respective equations can be found in *Andrews et al.* [1987].

The TEM equation provides a wave-mean flow theoretical framework for the dynamics of the stratosphere by connecting the change of the circulation to wave forcing [*Andrews et al.*, 1987]. In spherical coordinates, it can be expressed as

$$\frac{\partial \bar{u}}{\partial t} = - \left(\frac{1}{a \cos \phi} (\bar{u} \cos \phi)_\phi - f \right) \bar{v}^* - \bar{u}_z \bar{w}^* + \frac{1}{\rho_0 a \cos \phi} \nabla \cdot \mathbf{F} + \bar{X} \quad (1)$$

where a is the mean radius of the Earth, ϕ is latitude, $\rho_0 = \rho_s \exp(-z/H)$ is the standard density in log-pressure coordinates, ρ_s is the sea-level reference density, z is the log-pressure height coordinate, H is the mean scale height ($\approx 7 \text{ km}$), f is the Coriolis parameter, the overbar denotes zonal average, and subscripts denote the derivatives with respect to the given variable. The first and second terms on the right-hand side of equation (1) represent acceleration associated with the residual mean meridional circulation (\bar{v}^*, \bar{w}^*) , where

$$\bar{v}^* = \bar{v} - \frac{1}{\rho_0} \left(\rho_0 \frac{\bar{v}'\theta'}{\theta_z} \right)_z \quad (2)$$

$$\bar{w}^* = \bar{w} + \frac{1}{a \cos \phi} \left(\cos \phi \frac{\bar{v}'\theta'}{\theta_z} \right)_\phi \quad (3)$$

where θ is potential temperature, \bar{v} and \bar{w} are the Eulerian mean meridional circulation, and prime denotes the departure from zonal mean. The third term in the right-hand side of equation (1) represents the divergence of the EP flux

$$\nabla \cdot \mathbf{F} = \frac{1}{a \cos \phi} \left(F^{(\phi)} \cos \phi \right)_\phi + F_z^{(z)} \quad (4)$$

where

$$F^{(\phi)} = \rho_0 a \cos \phi \left(\frac{\bar{v}'\theta'}{\theta_z} \bar{u}_z - \bar{v}'u' \right) \quad (5)$$

$$F_z^{(z)} = \rho_0 a \cos \phi \left[\left(f - \frac{1}{a \cos \phi} (\bar{u} \cos \phi)_\phi \right) \frac{\bar{v}'\theta'}{\theta_z} - \bar{w}'u' \right] \quad (6)$$

and $\mathbf{F} = (F^{(\phi)}, F^{(z)})$ is the EP flux vector, which consists of a meridional component ($F^{(\phi)}$) that is related to poleward eddy momentum flux ($\bar{v}'u'$) and a vertical component ($F^{(z)}$) that is related to poleward eddy heat flux ($\bar{v}'T'$). As a whole, equation (1) states that the temporal change of the zonal mean zonal wind \bar{u} is affected by the Coriolis acceleration acting on the residual mean meridional circulation, upwelling/downwelling induced by vertical wind shear, the planetary wave drag that drives the circulation to departure from its radiative equilibrium, and the contribution from other nonconservative processes including gravity wave drag (the X term). We shall examine the meridional circulation term $\Theta = -\left(\frac{1}{a \cos \phi} (\bar{u} \cos \phi)_\phi - f \right) \bar{v}^* - \bar{u}_z \bar{w}^*$ and the EP flux divergence term $\Psi = \frac{1}{\rho_0 a \cos \phi} \nabla \cdot \mathbf{F}$.

The spherical form of the quasi-geostrophic refractive index squared can be estimated as

$$n_k^2(\phi, z) = \frac{\bar{q}_\phi(\phi, z)}{\bar{u}(\phi, z)} - \left(\frac{k}{a \cos \phi} \right)^2 - \left(\frac{f}{2N(z)H} \right)^2 \quad (7)$$

where

$$\bar{q}_\phi(\phi, z) = \frac{2\Omega \cos \phi}{a} - \frac{1}{a^2} \left(\frac{(\bar{u} \cos \phi)_\phi}{\cos \phi} \right)_\phi - \frac{f^2}{\rho_0} \left(\rho_0 \frac{\bar{u}_z}{N^2} \right)_z \quad (8)$$

and

$$-\frac{f^2}{\rho_0} \left(\rho_0 \frac{\bar{u}_z}{N^2} \right)_z = \left(\frac{f^2}{HN^2} + \frac{f^2}{N^2} \frac{dN^2}{dz} \right) \bar{u}_z - \frac{f^2}{N^2} \bar{u}_{zz} \quad (9)$$

where \bar{q}_ϕ is latitudinal gradient of the zonal mean potential vorticity, k is the spherical integer zonal wave number, $N(z)$ is the buoyancy frequency, and Ω is the Earth's rotation frequency. Planetary waves propagate in regions where $n_k^2 > 0$ and are evanescent in regions where $n_k^2 < 0$. To provide additional information on the dominant process(es) that lead to changes in planetary wave propagation, the relative contribution from the zonal wind strength \bar{u} , the meridional shear term $-\frac{1}{a^2} \left(\frac{(\bar{u} \cos \phi)_\phi}{\cos \phi} \right)_\phi$, the vertical shear term $\left(\frac{f^2}{HN^2} + \frac{f^2}{N^2} \frac{dN^2}{dz} \right) \bar{u}_z$, and the vertical curvature term $-\frac{f^2}{N^2} \bar{u}_{zz}$ are also examined separately.

Linear correlation and composite analyses are employed. The statistical significances of the composite differences are tested using the standard Student's t test. Whenever a p -value ≤ 0.05 is achieved over a relatively large area or region, the correlations or the composite differences estimated for the region are regarded as statistically significant. To investigate the temporal evolution of the signal, a running composite analysis is performed for a sequence of overlapping 31 day intervals with a forward step of 1 day for the extended NH winter period from October to March. All the composite differences presented hereafter are based on the results for eQBO-wQBO, so that the anomalies represent eQBO-related perturbations away from the state associated with wQBO. Also, the definition of a winter is based on January, e.g., the December–February mean of the 1958/1959 winter is numbered as 1959 in a time series plot. As a result, the winters of 1977–1997 studied by Lu *et al.* [2008] will be mentioned as 1978–1997 hereafter.

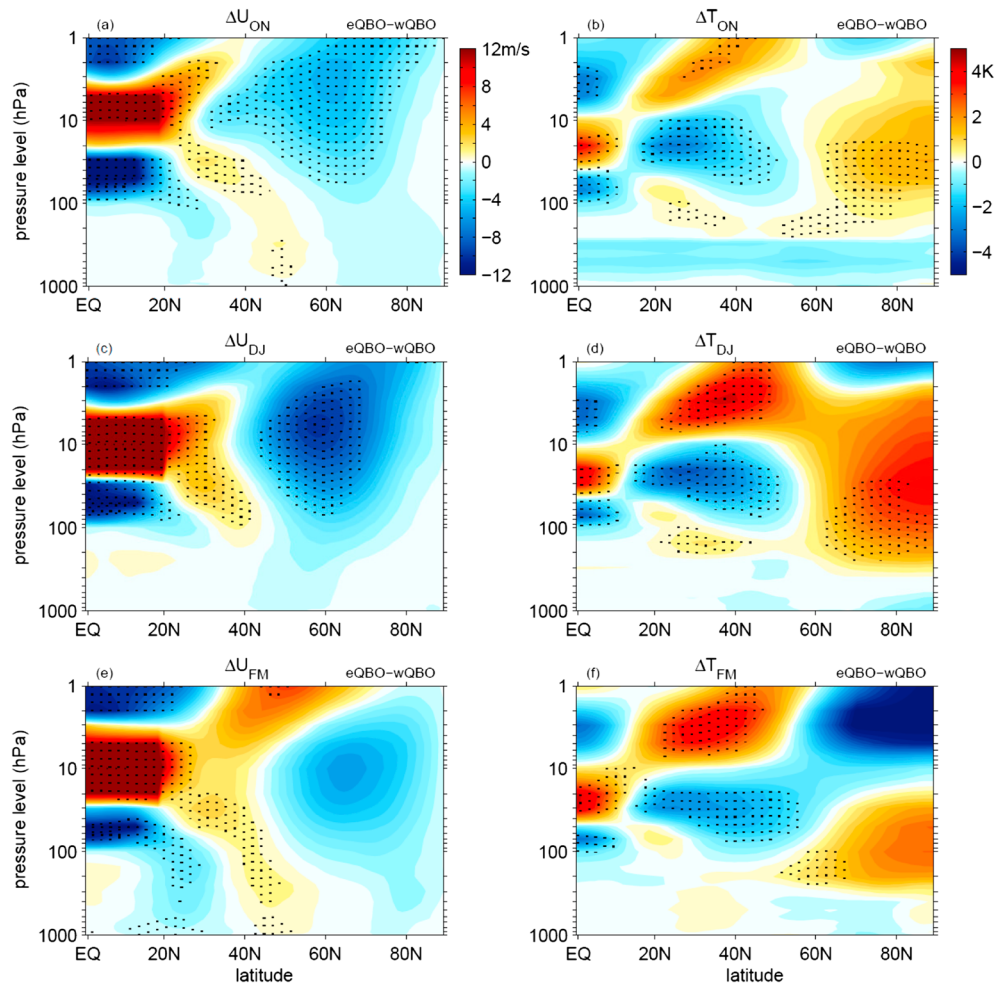


Figure 1. Latitude–height cross section of the composite differences between eQBO and wQBO (eQBO – wQBO) for (a, c, e) zonal mean zonal wind and (b, d, f) zonal mean temperature for October–November (ON), December–January (DJ), and February–March (FM) averages. The stippled areas indicate that the differences are statistically significant from zero at the $p = 0.05$ level. The winters affected by major volcanic eruptions are excluded. Similar results can be obtained when major warm ENSO affected winters are excluded.

The anomalous warming caused by volcanic aerosols in the stratosphere may contaminate the results. To examine the sensitivity of the result to such a contamination, the same analyses were performed both including and excluding the 24 months following major eruptions (i.e., Agung in March 1963, El Chichón in March 1982, and Pinatubo in June 1991). For the composite difference plots, we only show the results in which the volcano-affected winters are excluded. Their effect can, however, still be viewed in the time series plots. ENSO also has an effect on the polar vortex, with a cold ENSO leading to vortex intensification and a warm ENSO leading to more SSWs [Garfinkel and Hartmann, 2008]. We assessed the effect of ENSO on the QBO signal by excluding and including the winters affected by the major ENSO events (1972–1973, 1982–1983, 1997–1998, and 2009–2010). We found that the results are not sensitive to the contaminations from the major volcanic eruptions and major ENSO events.

3. Results

3.1. The HT Effect and Its Decadal Variation

Figure 1 shows the QBO composite differences (eQBO – wQBO) of zonal mean zonal wind (Figures 1a, 1c, and 1e) and temperature (Figures 1b, 1d, and 1f) for October–November (Figures 1a and 1b), December–January (Figures 1c and 1d), and February–March (Figures 1e and 1f) averages. The results are based on the merged ECMWF data for the period of 1958–2011. Similar results can be obtained by only using ERA-40 or ERA-Interim

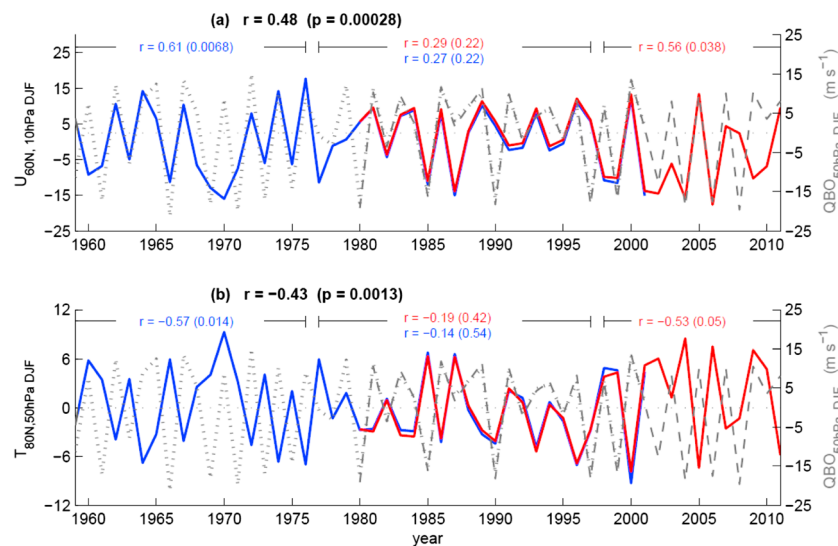


Figure 2. Time series of December–February mean (a) zonal mean zonal wind at 60°N, 10 hPa, and (b) and temperature anomalies at 80°N, 100 hPa, against December–February mean QBO. The blue lines are polar anomalies estimated from ERA-40, while the red lines are ERA-Interim polar anomalies. The dotted and dashed gray lines are the 50 hPa QBO estimated from ERA-40 and ERA-Interim, respectively. The correlation coefficients and the p -values (in brackets) for the entire period of 1959–2011 are given at the top of each subplot together with those for the three subperiods of 1959–1976, 1978–1997, and 1999–2011.

alone, and with or without the winters affected by major volcanic eruption and/or major warm ENSO events, suggesting that the HT effect and its seasonal progression are robust features in NH winter.

In the high-latitude stratosphere, the HT effect is marked by easterly anomalies and a warmer pole region at 20–200 hPa in association with the eQBO in the lower stratosphere. The magnitude of the signal is the largest in midwinter (December–January), while the areal extent of the HT effect is largest in early winter (October–November). The HT effect becomes much weaker in late winter (February–March) when a significant high-latitude response is only found in temperature and the signal is confined to a small region near 60°N, 100–200 hPa.

In the tropical and subtropical stratosphere, the impact of the QBO-induced meridional circulation is clearly evident. It is marked by the three-vertical-cell structure of the temperature anomalies both at the equator and in the subtropics. An eQBO in the lower stratosphere corresponds to a vertically sheared tropical wind structure with an easterly shear near 5 hPa and a westerly shear near 20–30 hPa. The easterly and westerly shear zones have cold and warm temperature anomalies, respectively. These temperature anomalies are maintained by the QBO-induced meridional circulation, with upwelling or subsidence at the equator and an opposite motion in the subtropics [Plumb and Bell, 1982]. Enhanced by the residual mean meridional circulation of the stratosphere, the QBO-induced meridional circulation intensifies and extends into the midlatitudes of the winter hemisphere. As a result, the temperature anomalies on the subtropical branches become larger than their tropical counterparts [Kinnersley and Tung, 1998]. To maintain thermal wind balance, the subtropical and the midlatitude zonal wind anomalies arch down toward the tropopause, as evident especially in October–November and February–March in Figure 1.

Figure 2 shows the time series of the December–February mean QBO (the dotted gray line from ERA-40 and the dashed gray line from ERA-Interim) against the zonal mean zonal wind anomaly at 60°N, 10 hPa (Figure 2a), and the zonal mean temperature anomaly at 80°N, 50 hPa (Figure 2b). For both the QBO and polar time series, it is clear that the two ECMWF data sets match each other very well for the common period 1979–2001. Similar results can be obtained for the other winter seasonal averages. Thus, the HT effect and its variation are not sensitive to the differences between the data sets.

For the entire period of 1958–2011, the correlation coefficients (r) between the QBO and the polar wind and temperature are 0.48 and -0.43 , both significant at $p \leq 0.01$. Slightly higher correlation coefficients (~ 0.55) are obtained for October–December and November–January averages, and lower correlation coefficients

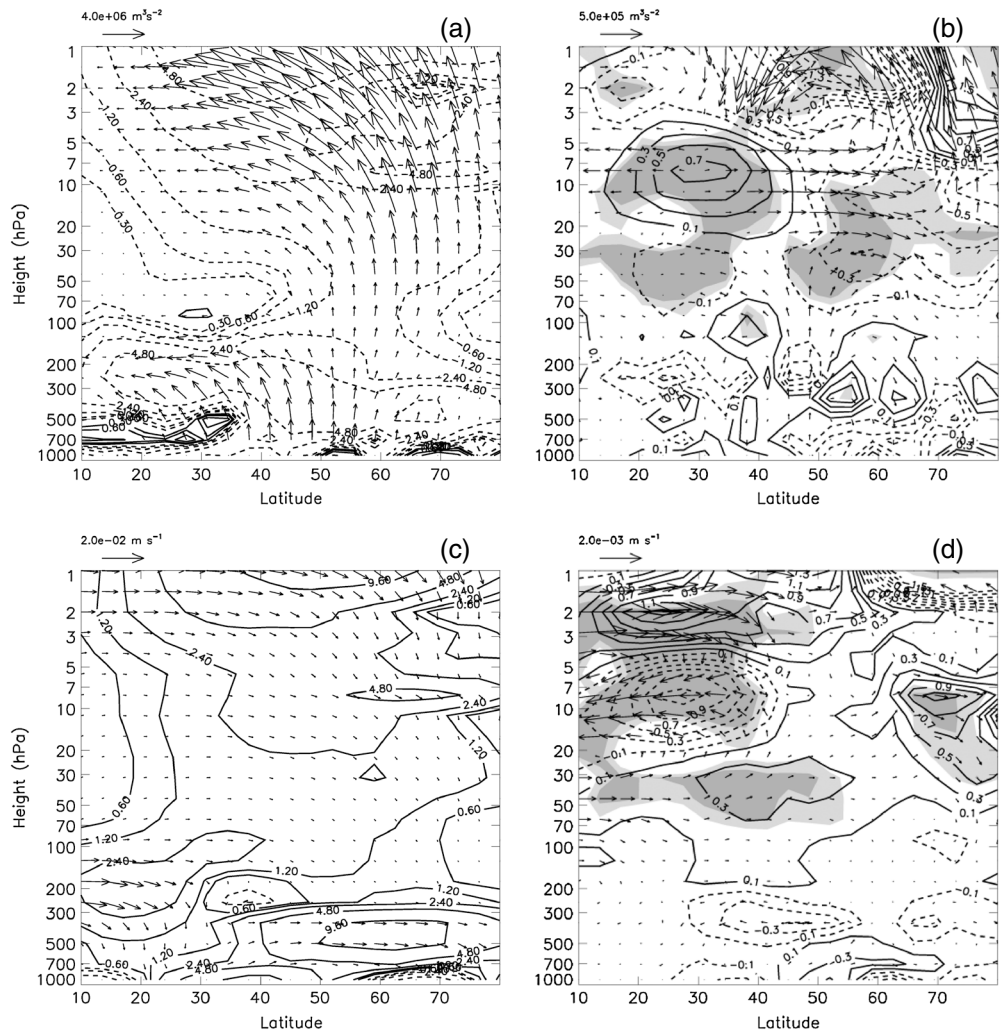


Figure 3. Latitude–height cross section of the December–February mean (a) climatology and (b) QBO composite differences (eQBO – wQBO) of the EP flux (arrows) and EP flux divergence term Ψ (contours). Solid and dashed contours are positive and negative divergence at the intervals of $\pm 0.6, \pm 1.2, \pm 2.4, \pm 4.8 \dots \times 10^{-5} \text{ m s}^{-2}$ for climatology and $\pm 0.1, \pm 0.3, \pm 0.5 \dots \times 10^{-5} \text{ m s}^{-2}$ for the difference plots. The light and dark shaded areas represent p -values equal to or smaller than 0.1 and 0.05, respectively. The EP flux vectors are scaled for a clearer visualization of planetary wave propagation in the stratosphere (see text for further details of the scaling). Latitude–height cross section of the December–February mean (c) climatology and (d) QBO composite differences (eQBO – wQBO) of the residual mean meridional circulation (arrows) and the residual circulation term Θ (contours). The contour interval and shading are the same as in Figures 3a and 3b.

(~ 0.35) are obtained for January–March averages. Very similar results can be obtained if the QBO leads the polar time series by 1 or 2 months.

The correlation coefficients of the three subperiods (1959–1976, 1978–1997, and 1999–2011) indicate a significant weakening of the HT effect during 1978–1997 as shown by Lu *et al.* [2008] who used the blended ERA-40 and ECWMF Operational data sets. This weakening held true for the polar wind and temperature over a large vertical range, and it was most severe in middle to late winter (January–March). In fact, the correlation coefficient in the midperiod has an opposite sign to those in the two ending subperiods when January–March averages are used (not shown, but the evidence has been given in Lu *et al.* [2008]).

3.2. Dynamical Mechanisms of the HT Effect

According to equation (1), detecting the changes in wave driving (i.e., EP flux divergence term Ψ) and the residual mean meridional circulation (i.e., the Θ term) can provide useful diagnostic information for

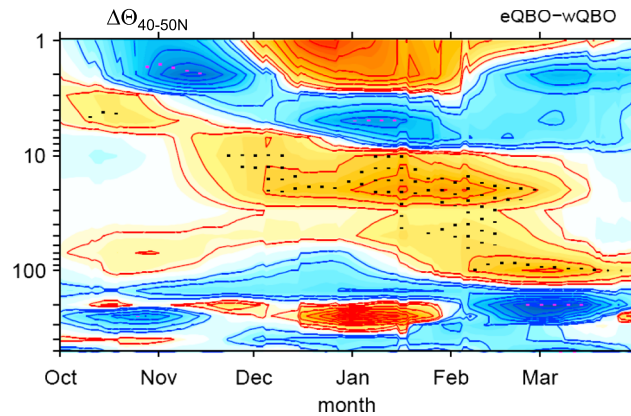


Figure 4. Time-height cross section of daily running QBO composite differences (eQBO – wQBO) of meridional circulation term Θ averaged for the latitude band of 35–50°N for the extended winter period (October–March). The contours are $\pm 0.25, \pm 0.5, \pm 1, \pm 2, \pm 4, \pm 8 \times 10^{-5} \text{ m s}^{-2}$. A 31 day average window is applied to both the QBO and Θ . The stippled areas indicate statistical significance (tested by Student’s t test) at the $p = 0.05$ level. The data affected by the three major volcano eruptions are excluded. Similar results can be obtained when major ENSO events are excluded as well.

understanding circulation changes in the stratosphere. Figures 3a and 3b show the climatology and the QBO composite differences of December–February mean EP fluxes (arrows) and EP flux divergence (contours). The vectors of $(F^{(\phi)}, F^{(z)})/\rho_0$ are plotted because $F^{(\phi)}$ and $F^{(z)}$ become vanishingly small with increased height due to the decrease in density. To better visualize the wave propagation in both vertical and horizontal directions, all vectors in Figure 3 are further scaled by the ratio between the vertical and horizontal distances on the plot. As a result of the scaling, the magnitude of the divergence field $\nabla \cdot \vec{F}$ cannot be directly inferred by the EP flux vectors. However, the Ψ contours are not scaled; they thus represent the true magnitude of wave forcing. Composite difference plots for other winter monthly or seasonal averages show similar features

to Figure 3b. Similar to Figure 1, there is a poleward movement and intensification of the subtropical anomalies that is accompanied by a poleward and downward propagation of the high-latitude anomalies from October to March (not shown).

During December–February, QBO modulation of the EP flux divergence is characterized by anomalous divergence in the subtropical midstratosphere and convergence at high latitudes, implying a poleward shift of planetary wave momentum deposition under eQBO. Negative anomalies of EP flux divergence appear in the subtropical lower and upper stratosphere. The magnitude of the lower and upper stratospheric anomalies is less than half of those at 20–5 hPa. In the midlatitudes, QBO modulation of the winter time EP fluxes is marked by upward EP flux anomalies from the troposphere into the stratosphere (35–50°N, 200–20 hPa) and poleward anomalies in the midstratosphere (35–60°N, 20–5 hPa). In the high latitudes, it is marked by upward anomalies at 65–80°N, 20–1 hPa, and equatorward anomalies at 35–60°N, 3–1 hPa. This implies anomalous wave convergence in the high-latitude stratosphere, and it is consistent with a weaker, warmer vortex under eQBO.

Figures 3c and 3d show the climatology and the QBO composite differences of December–February mean residual mean meridional circulation (\bar{v}^*, \bar{w}^*) (arrows) and the residual mean meridional circulation term Θ (contours). QBO modulation of the residual mean meridional circulation is marked by the following: (1) positive Θ anomalies in the midlatitude lower stratosphere, indicating a stronger meridional circulation under eQBO in the region; (2) a dipole pattern at 20–5 hPa with negative Θ anomalies in the subtropics and positive Θ anomalies in the polar stratosphere; and (3) a similar but opposite-signed dipole pattern in the uppermost stratosphere. The three-vertical-cell structure in the subtropics to midlatitudes corresponds well to the vertically sheared QBO structure in the tropics (see Figure 1); it is known to be associated with the QBO-induced meridional circulation [Plumb and Bell, 1982; Andrews et al., 1987]. An overall strengthening of the residual mean meridional circulation in the stratosphere is associated with eQBO compared to wQBO.

Over monthly or seasonal time scales, $\partial \bar{u} / \partial t$ is normally about two orders smaller than the two other terms; thus, Θ and Ψ should balance each other (see equation (1)) [see also Newman et al., 2001]. This holds roughly true for the climatology as well as the difference plots in the middle to lower stratosphere. The Θ anomalies are generally larger than those of Ψ in the subtropics while they become more comparable in magnitude in the midlatitudes and over the polar region. In the subtropics, larger Θ anomalies are expected because the QBO directly affects the meridional circulation [Plumb and Bell, 1982] while the QBO effect on the planetary wave forcing is most likely indirect [Holton and Tan, 1980; Garfinkel et al., 2012]. The large contribution from

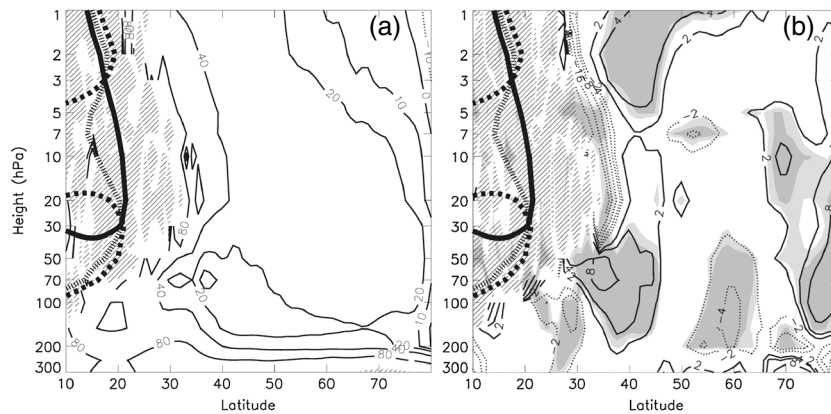


Figure 5. Latitude-height cross section of the December–February mean (a) climatology and (b) QBO composite differences (eQBO – wQBO) of the refractive index n^2 scaled by multiplying it by a^2 . Solid and dashed contours are positive and negative values at the intervals of $\pm 10, \pm 20, \pm 40, \pm 80, \dots$ for climatology and $\pm 2, \pm 4, \pm 8, \pm 16, \dots$ for the difference plot. The thick solid, dashed, and dotted lines are the mean zero wind lines for the wQBO, eQBO, and climatology conditions. The regions where $(an)^2 < -20$ or > 160 are indicated by hatching in climatology, and the regions where $(an)^2 > 64$ are indicated by hatching in the difference plot.

the residual mean meridional circulation in the upper stratosphere implies that a change of wave driving alone is not adequate to explain the circulation change in this region. Other contributors in addition to planetary wave forcing are important here, most likely the contribution from gravity wave drag.

The temporal evolution of the Θ anomalies in the midlatitude stratosphere is shown in Figure 4. A significant positive Θ anomaly appears first in the upper stratosphere in October, then descends into the midstratosphere in November, and finally descends into the lower stratosphere in February and March. Thus, a stronger meridional circulation is associated with eQBO as compared to wQBO, consistent with Figure 3d. The negative Θ anomaly above the positive one can be understood as reduced planetary wave propagation at a higher level because of more planetary wave breaking below.

Figure 5 shows the climatology and the QBO composite difference of December–February mean refractive index n^2 for zonal wave number 1 quasi-stationary waves, where n^2 is multiplied by the square of the Earth's radius a^2 . Note that the second and third terms on the right-hand side of equation (7) tend to cancel out in the composite difference plot, so any significant n^2 anomaly in a difference plot mainly reflects a variation of \bar{q}_ϕ/\bar{u} .

In the lower stratosphere and upper troposphere, the QBO signal in n^2 is marked by positive n^2 anomalies at 30–45°N and negative anomalies at 20–30°N and at 55–65°N. These wave guide anomalies are in good agreement with the EP flux anomalies in the associated regions (Figure 3b). The positive n^2 anomaly at 30–45°N is collocated with equatorward propagating EP flux anomalies in the same region. These anomalies lead to the EP flux convergence anomalies at 20–35°N. The negative n^2 anomalies in the subtropics and the positive n^2 anomalies in the midlatitudes are consistent with a poleward shift of the quasi-stationary wave guide in association with the subtropical critical line under eQBO. However, the alternating negative, positive, and negative n^2 anomalies and the associated EP flux anomalies in the lower stratosphere are inconsistent with what we would expect if the critical-line mechanism was the major factor driving the HT effect.

In the subtropical middle stratosphere, a narrow vertical belt of negative n^2 anomalies can be found at ~35°N, 30–5 hPa. The magnitude of the anomalies is about half of the climatological value in the same region. It is associated with the enhanced poleward EP flux propagation at 35–60°N (see Figure 3b) and an enhanced meridional circulation in the midlatitude middle to lower stratosphere (see Figure 4). An enhanced poleward wave refraction in the midstratosphere is inconsistent with the critical-line effect at 20–5 hPa where the equatorial zero wind line is located in the southern hemisphere; fewer planetary waves should be able to propagate toward the winter pole. These negative n^2 anomalies are, however, consistent with the QBO-induced meridional circulation mechanism in terms of their location and effect on the EP fluxes [Garfinkel et al., 2012], thus suggesting that the influence of the QBO-induced meridional circulation is the primary influence while the subtropical critical-line effect plays a less important role.

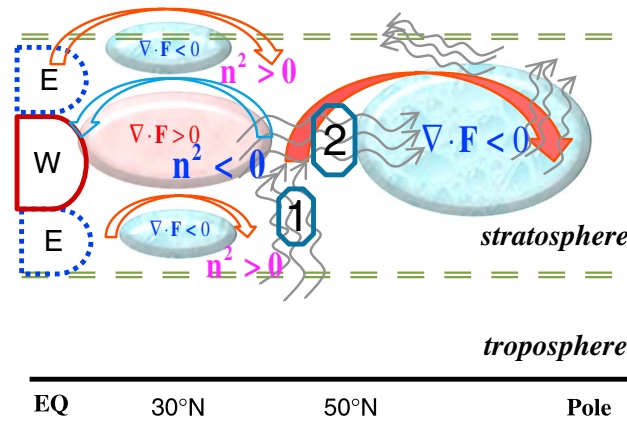


Figure 6. Schematic diagram of the QBO modulated anomalies of the EP flux divergence (shaded ovals), the residual mean meridional circulation (double-lined arrows), the refractive index (n^2), and planetary wave propagation. The vertical structure of the equatorial QBO zonal wind anomalies is given on the left. The red and blue colors represent positive and negative anomalies, respectively. The gray arrows indicate the direction of the anomalous planetary wave propagation. The green dashed lines represent the tropopause and stratopause. See text for further details. The two numbers where anomalous wave propagation are identified are investigated in more detail in section 3.2.

In the upper stratosphere, positive n^2 anomalies appear at 30–45°N, associated with a slightly poleward shift of the critical line. The magnitude of the anomalies is only ~10% of the climatological value in the region, much smaller than those in the middle and lower stratosphere. Nevertheless, these upper level n^2 anomalies are consistent with more EP fluxes being refracted toward the region from high latitudes and consequently the enhanced EP flux convergence at 15–25°N, 2 hPa (see Figure 3b). If the critical-line mechanism held, we would expect a poleward shift of the wave forcing under eQBO. However, what we have found is more planetary waves propagating from the high latitudes toward the subtropics; this is opposite to what we would expect from the critical-line effect. This suggests that the critical-line mechanism does not play an important role in regions other than the subtropical lower stratosphere.

In the polar stratosphere, the n^2 anomalies are largely positive. As they are a direct result of the weaker \bar{u} in the region under eQBO conditions, they are a reflection of the HT effect itself and cannot be used to establish causality.

To understand how the QBO-induced meridional circulation affects the subtropical to midlatitude n^2 , we examine the individual contributions from the zonal wind term $\frac{2\Omega \cos \phi}{a\bar{u}}$, meridional shear term $-\frac{1}{a^2\bar{u}} \left(\frac{\bar{u} \cos \phi}{\cos \phi} \right)_{\phi}$, vertical shear term $\left(\frac{f^2}{HN^2} + \frac{f^2}{N^2} \frac{dN^2}{dz} \right) \frac{\bar{u}_z}{\bar{u}}$, and vertical curvature term $-\frac{f^2}{N^2} \frac{\bar{u}_{zz}}{\bar{u}}$ (see equations (7)–(9)). We find that, in general, the anomalies associated with the three derivative terms are not sensitive to the values of \bar{u} at 30–45°N. At 35–50°N, the negative n^2 anomalies at 20–5 hPa are mainly controlled by the meridional as well as the vertical derivative terms. Below 20 hPa, \bar{u} becomes more important. The positive n^2 anomalies in the upper troposphere and lower stratosphere are mainly due to the vertical curvature of the mean flow. Because of the importance of the derivative terms, a QBO modulation of the EP fluxes in the key region of 35–50°N, 20–5 hPa, is associated with a change of flow geometry in both vertical and horizontal directions. As proposed by Garfinkel *et al.* [2012], the changes are more likely to be associated with the QBO-induced meridional circulation rather than the subtropical critical-line effect.

Figure 6 summarizes how a QBO modulation of the planetary waves can cause the observed HT effect. It is essentially adapted from the diagrams of Yamashita *et al.* [2011] and Garfinkel *et al.* [2012] with some minor modifications. The QBO-induced meridional circulation anomalies (indicated by the three double arrows near the subtropics) extend from the subtropics to the midlatitudes during winter. The poleward movement of the QBO-induced meridional circulation causes a change in the mean flow geometry in the midlatitude stratosphere. Under eQBO, this leads to the formation of a midlatitude wave guide that enhances both the upward propagation of planetary waves from the troposphere into the lower stratosphere at 35–50°N, 50–200 hPa, and the northward wave propagation at ~35°N, 5–50 hPa (indicated by the $n^2 < 0$). This anomalous wave guide leads to more planetary waves (indicated by the thin, grouped arrows) propagating into an EP flux convergence region in the polar stratosphere (indicated by the blue oval with $\nabla \cdot F < 0$) and diverging in the subtropical middle stratosphere (indicated by the red oval with $\nabla \cdot F > 0$). According to the “downward-control” principle [Haynes *et al.*, 1991], stronger planetary wave driving in the middle to high latitudes enhances the residual mean meridional circulation at and below the forcing region (indicated by the red and solid poleward double arrow), therefore leading to a more disturbed polar vortex and a warmer polar

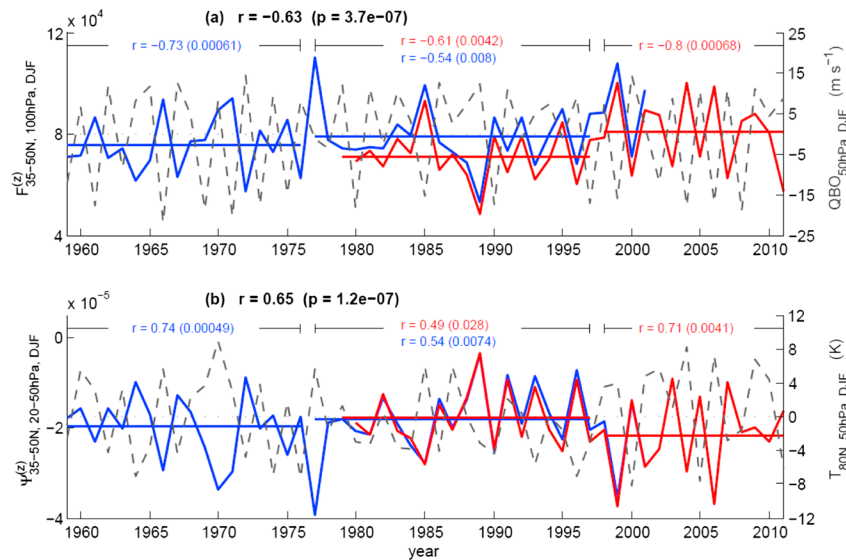


Figure 7. (a) Time series of the December–February mean upward EP flux $F^{(z)}$ (solid lines) at 35–50°N, 100 hPa, against the December–February mean QBO (dashed line). (b) Time series of the December–February mean vertical component of EP flux divergence $\Psi^{(z)}$ at 35–50°N, 50–20 hPa, against the zonal mean polar temperature at 80°N, 50 hPa. The horizontal solid lines indicate the average value for a given subperiod and data set. The line colors, correlation coefficients, and p -values are as described in the caption for Figure 2.

lower stratosphere. The anomalous convergence zones in the subtropical lower and upper stratosphere (indicated by the two small-sized blue ovals) are directly associated with the QBO-induced meridional circulation; they, however, play a minor role in explaining the HT effect.

3.3. Cause of the HT Effect Weakening During 1978–1997

The weakening of the HT effect during 1978–1997 could be due to either a decadal-scale variation of the tropospheric wave forcing (source related) or a change of the background flow through which the planetary waves travel (propagation related). In the context of stratospheric QBO modulation of planetary waves and the HT effect, the latter would most likely involve a change of circulation in the stratosphere. In this section, we evaluate these two possibilities.

To examine whether or not planetary waves behaved differently during 1978–1997, we target two regions, indicated by the bold numbers 1 and 2 in Figure 6. These two regions are selected because they represent the most important gateways for QBO modulation of planetary wave propagation in the midlatitudes (Figure 3b). Upward EP fluxes are enhanced under eQBO in region #1, where a corresponding decadal-scale variation of tropospheric planetary waves may be important. Poleward EP fluxes are enhanced under eQBO in region #2, where a variation of stratospheric circulation may play a role.

Figure 7a shows the time series of December–February mean upward EP flux at 35–50°N, 100 hPa ($F_{35-50N,100hPa}^{(z)}$), against the December–February mean QBO. Figure 7b shows the vertical component of the EP flux divergence at 35–50°N, 20–50 hPa ($\Psi_{35-50N,20-50hPa}^{(z)}$), against the zonal mean polar temperature at 80°N, 50 hPa ($T_{80N,50hPa}$), for the same midwinter months. $F_{35-50N,100hPa}^{(z)}$ and $\Psi_{35-50N,20-50hPa}^{(z)}$ are negatively correlated with $r = -0.95$, implying a larger poleward heating flux from the troposphere into the lower stratosphere is directly associated with a stronger wave forcing just above the forcing level. Thus, $F_{35-50N,100hPa}^{(z)}$ and $\Psi_{35-50N,20-50hPa}^{(z)}$ are effectively interchangeable despite having the opposite sign.

$F_{35-50N,100hPa}^{(z)}$ is negatively correlated with the QBO, implying that stronger upward wave forcing from the troposphere is associated with eQBO, while weaker forcing is associated with wQBO. Similar correlations can be obtained at pressure levels in the region 70–200 hPa, but the relationship breaks down at lower levels in

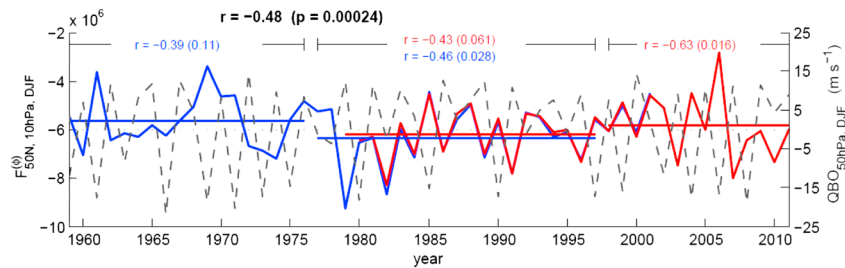


Figure 8. Time series of the December–February mean horizontal EP flux $F_{50N,10hPa}^{(\phi)}$ (solid colored lines) at 50°N, 10 hPa, against the December–February mean QBO (dashed line). The line colors, correlation coefficients, and p -values are as described in the caption for Figure 2.

the troposphere. This implies that the modulation is mainly associated with a change of wave guide near the subtropical lower stratosphere rather than a direct QBO effect on the upward eddy flux in the troposphere. Note also that $\Psi_{35-50N,20-50hPa}^{(z)}$ and $T_{80N,50hPa}$ are positively correlated, implying that the polar temperature in the lower stratosphere is higher with a stronger wave forcing. Together, they suggest that the polar temperature is negatively correlated with the QBO, which is consistent with the HT effect. For the entire period of 1958–2011, the correlation coefficients are ~ 0.65 , significant at $p < 0.001$. These results suggest that there is a dynamically consistent link between the QBO, the EP fluxes, and the temperature in the polar lower stratosphere.

A closer inspection of the temporal variation of the time series suggests that there was no sudden decrease or increase of $F_{35-50N,100hPa}^{(z)}$ around 1976/1977 and 1997/1998 winters in the ERA40 estimates (blue line) while there was an upward jump of $F_{35-50N,100hPa}^{(z)}$ around 1997 in the ERA-Interim estimates (red line). $F_{35-50N,100hPa}^{(z)}$ from ERA-40 and ERA-Interim match each other very well in terms of their interannual variation, but the ERA-40 estimates are consistently larger than those from ERA-Interim for the common period of 1979–2001. This cross-data-set difference makes it harder to tell whether or not a change of planetary wave activity from the troposphere occurred around 1976 and 1997.

The cross-data-set difference is much reduced in $\Psi_{35-50N,20-50hPa}^{(z)}$ as the errors in the baseline of $F^{(z)}$ are cancelled out when a difference operator is applied to the adjacent vertical levels. An upward shift in $\Psi_{35-50N,20-50hPa}^{(z)}$ was apparent in 1978–1997, implying reduced wave convergence in the lower stratosphere. Furthermore, the correlation coefficient during 1978–1997 was lower than those in the earlier and later subperiods, consistent with the weakened HT effect during the time. However, these differences are too small to fully explain the significant drop of correlation between the QBO and $T_{80N,50hPa}$ during 1978–1997 (Figure 2). Also, a reduction of $\Psi_{35-50N,20-50hPa}^{(z)}$ does not mean a reduction of the wave forcing at the source region where the planetary waves are generated, as a change of stratospheric circulation can also cause a reduction of $\Psi_{35-50N,20-50hPa}^{(z)}$.

Figure 8 shows the time series of December–February mean horizontal EP flux at 50°N, 10 hPa ($F_{50N,10hPa}^{(\phi)}$) against the December–February mean QBO. Note that ERA-40 and ERA-Interim give nearly identical results for their common period. Qualitatively similar results can be obtained anywhere within the latitude band of 35–60°N.

This figure shows that $F_{50N,10hPa}^{(\phi)}$ is negatively correlated with the QBO, implying that stronger poleward propagating EP fluxes are associated with eQBO, while stronger equatorward propagating EP fluxes are associated with wQBO. This is consistent with Figure 3b. The correlation coefficient is 0.48 and is significant at $p < 0.001$. There was an enhancement of equatorward EP flux propagation during 1978–1997. However, the correlation between $F_{50N,10hPa}^{(\phi)}$ and the QBO strengthens with time but with no sign of a change of correlation during 1978–1997. Thus, it is not evident that a decadal variation of QBO modulation of the eddy momentum flux in region #2 caused the weakening of the HT effect in 1978–1997.

Figures 7 and 8 suggest that QBO modulation of the EP fluxes and EP flux divergence did not change notably during 1978–1997 as compared to the earlier and later subperiods. It is possible that other processes might have interfered with QBO modulation of the wave propagation in nearby regions. Figure 9 shows a latitude-height

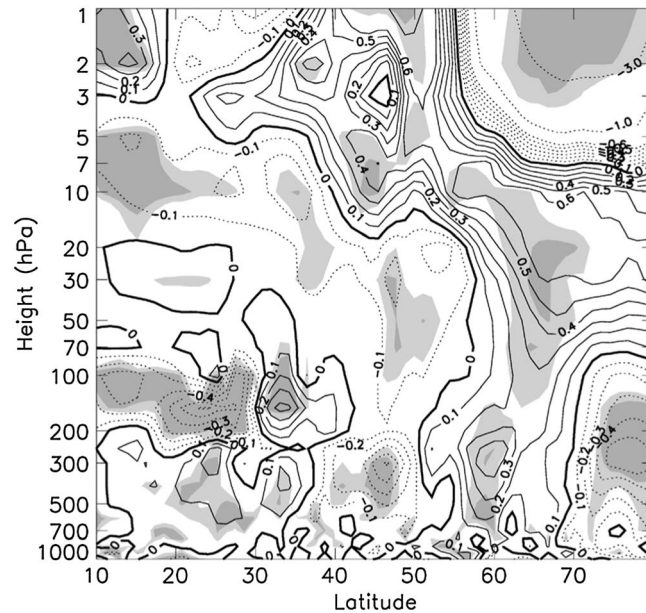


Figure 9. Latitude–height cross section of the composite differences of the December–January mean horizontal EP flux divergence term $\Psi^{(\phi)}$ between the midperiod (1978–1997) and the earlier and later periods (1959–1976 + 1999–2011). The contours are $\pm 0.1, \pm 0.2, \pm 0.3, \dots$ linearly up to $0.6 \times 10^{-5} \text{ m s}^{-2}$ and then $\pm 1, \pm 3 \times 10^{-5} \text{ m s}^{-2}$ thereafter. The thicker line indicates zero difference. The shadings are as described in the caption for Figure 3.

cross section of the composite differences of December–February mean $\Psi^{(\phi)}$ between 1978–1997 and the earlier and later subperiods. It is evident that positive $\Psi^{(\phi)}$ anomalies appear near the peak axis of the polar vortex, where the westerly winds are the strongest. Negative $\Psi^{(\phi)}$ anomalies appear in the surrounding regions where the westerly winds are relatively weaker. This effect even extends into the troposphere at $\sim 60^\circ\text{N}$. These $\Psi^{(\phi)}$ anomalies indicate that planetary waves were more likely to be refracted away from the axis of the vortex during 1978–1997, which is counter to QBO modulation of planetary waves in the subtropical to midlatitude stratosphere (see Figure 3b) and would lead to a disruption of the QBO effect on wave driving and a weakening of the HT effect.

Qualitatively similar results to those shown in Figure 9 can be obtained based on either ERA-40 or ERA-Interim data. No coherent changes can, however, be detected when $\Psi^{(\phi)}$ is replaced by the total EP flux divergence Ψ or its vertical component $\Psi^{(z)}$ (not shown). This is partly due to the large difference in $\Psi^{(z)}$ between the two data sets as the differences between the two ECMWF data sets are negligibly small for the horizontal EP flux but significantly larger for the vertical EP flux. The detectable upward baseline shift in the ERA-40 reanalysis of the vertical EP flux compared to that of ERA-Interim may also indicate a warmer bias of the stratosphere in the ERA-40 reanalysis.

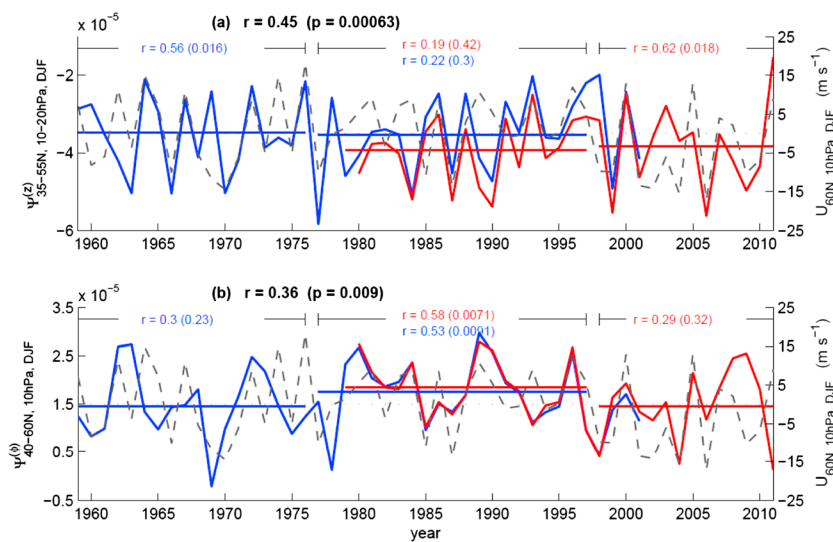


Figure 10. (a) Time series of the December–February mean vertical EP flux divergence term $\Psi^{(z)}$ (solid lines) at $35\text{--}55^\circ\text{N}$, $10\text{--}20 \text{ hPa}$, against the zonal mean zonal wind at 60°N , 10 hPa (dashed line). (b) Time series of the December–February mean horizontal EP flux divergence term $\Psi^{(\phi)}$ at $40\text{--}60^\circ\text{N}$, 10 hPa . The line colors, correlation coefficients, and p -values are as described in the caption for Figure 2.

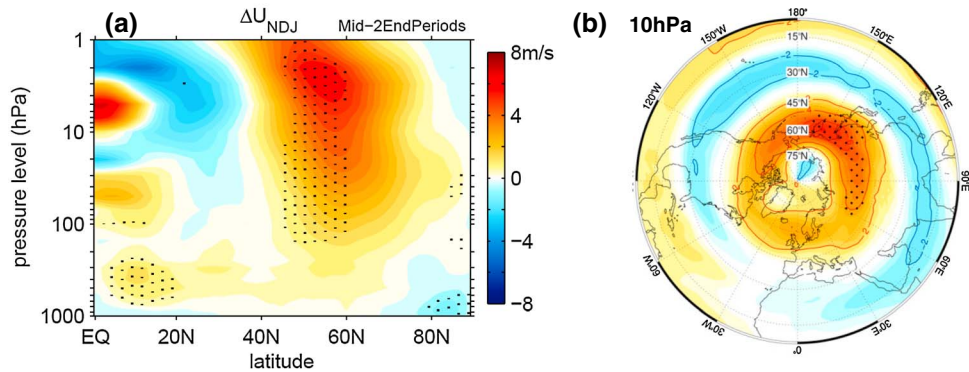


Figure 11. (a) Latitude–height cross section of the November–January mean composite differences in the zonal mean zonal wind between the midperiod (1978–1997) and the earlier and later periods (1959–1976 + 1999–2011) zonal mean. (b) The same composite differences as in Figure 11a but for a polar plot at 10 hPa. The stippled areas indicate statistical significance (tested by Student’s *t* test) at the $p=0.05$ level.

Figure 10 shows the temporal evolution of the 1978–1997 disruption around the peak axis of the polar vortex. It shows the vertical EP flux divergence term at 35–55°N, 10–20 hPa, $\Psi_{35-55N,10-20hPa}^{(z)}$ (Figure 10a), and the horizontal component of the EP flux divergence at 40–60°N, 10 hPa, $\Psi_{40-60N,10hPa}^{(\phi)}$ (Figure 10b), both against the zonal mean zonal wind at 60°N, 10 hPa, $U_{60N,10hPa}$. Again, all the time series are of December–February means. The magnitude of $\Psi_{35-55N,10-20hPa}^{(z)}$ is about twice as large as that of $\Psi_{40-60N,10hPa}^{(\phi)}$ on average, implying that the vertically propagating planetary waves induced by the eddy heat fluxes $\overline{v'T'}$ are the dominant wave forcing in the region. The strength of the polar vortex is positively correlated with $\Psi_{35-55N,10-20hPa}^{(z)}$ and $\Psi_{40-60N,10hPa}^{(\phi)}$, implying that a stronger wave forcing (i.e., more negative $\Psi_{35-55N,10-20hPa}^{(z)}$) near the vortex peak axis is associated with a weaker polar vortex. During 1959–1976 and 1999–2011, the correlations between $U_{60N,10hPa}$ and $\Psi_{35-55N,10-20hPa}^{(z)}$ were statistically significant, but the relationship disappeared during 1978–1997. Instead, a significant correlation

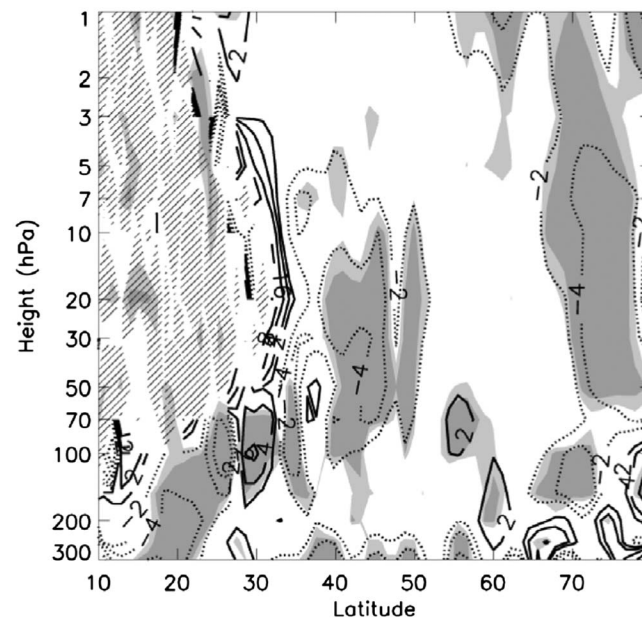


Figure 12. Latitude–height cross section of the November–January mean composite differences of the refractive index n^2 between the midperiod (1978–1997) and the earlier and later periods (1959–1976 + 1999–2011). The scaling, contour intervals, shadings, and hatching are as described in the caption for Figure 5b.

between $\Psi_{40-60N,10hPa}^{(\phi)}$ and $U_{60N,10hPa}$ was found in 1978–1997, but it was not significant during the earlier and later subperiods. Also, the average value of $\Psi_{40-60N,10hPa}^{(\phi)}$ was significantly more positive during 1978–1997, implying anomalous wave divergence during the period. Because vertical EP flux is the dominant wave forcing in the region, this change of behavior in the link of the strength of the vortex to the vertical and horizontal components of the EP flux divergence terms suggests the following: (1) during the earlier and later subperiods, the planetary wave forcing from below weakened the polar vortex; and (2) in 1978–1997, the polar vortex ducted the waves away from its peak axis (see also Figure 9).

Figure 11 suggests that the polar vortex was broadened equatorward in the lower stratosphere and strengthened in the middle to upper stratosphere during 1978–1997 in November–January

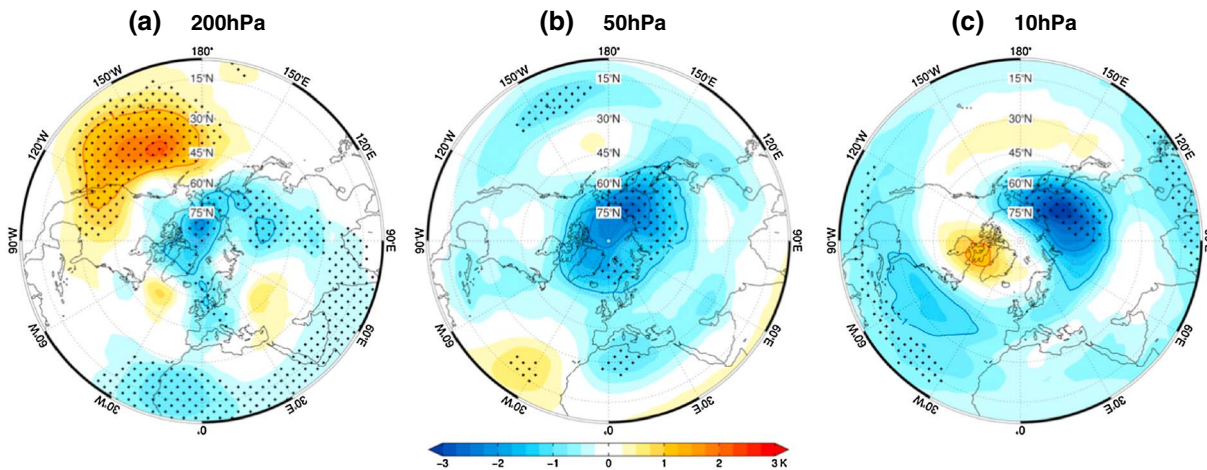


Figure 13. Polar plots of November–January mean temperature composite differences between the midperiod (1978–1997) and the earlier and later periods (1959–1976 + 1999–2011) at (a) 200 hPa, (b) 50 hPa, and (c) 10 hPa. The stippled areas indicate statistical significance (tested by Student’s *t* test) at the $p=0.05$ level.

compared to the earlier and later subperiods. The 1 month lag between this analysis and the analyses of QBO modulation of the EP fluxes accounts for the preconditioning of the stratospheric background flow. Figure 11b also indicates that the significant strengthening of the polar vortex at 10 hPa was mostly confined to the west Pacific and northeastern Asia.

Figure 12 shows the composite difference of November–January mean refractive index n^2 between the midperiod (1978–1997) and the earlier and later periods (1959–1976 + 1999–2011). As in Figure 5, n^2 is scaled by the square of the Earth’s radius a^2 and it is for zonal wave number 1 quasi-stationary waves. The anomalous behavior of n^2 in the midperiod 1978–1997 was marked by negative n^2 anomalies at 35–50°N in the lower to middle stratosphere, at 65–75°N, 1–70 hPa, and at 15–25°N in the upper troposphere. When isolating the contribution of each term constituting the refractive index n^2 , we find that the negative n^2 anomalies in the high-latitude stratosphere were induced by the broadened and strengthened polar vortex that gave rise to a reduction of latitudinal gradient of the zonal mean potential vorticity \bar{q}_ϕ inside the vortex. The negative n^2 anomalies at 35–50°N were mainly controlled by the meridional wind curvature $\left(\frac{\bar{u} \cos \phi}{\cos \phi}\right)_\phi$, while both the vertical wind shear and meridional wind curvature were responsible for the negative anomalies in the subtropical upper troposphere (see equation (8)). Compared with Figure 5b, it is clear that these wave guide anomalies generally had an opposite sign to the QBO modulation of n^2 . The negative n^2 anomalies in the subtropical to midlatitude lower stratosphere imply that it was reduced wave propagation into the QBO affected regions that led to a reduced sensitivity to the QBO during the period 1978–1997. However, the eddy heat fluxes estimated at 100 hPa from ERA-40, ERA-Interim, or the combined data set do not suggest that there was a significant reduction of wave forcing from the troposphere during this period. Thus, it is unlikely that the broadening and strengthening of the polar vortex were linked to a reduction of the planetary wave forcing from the troposphere; it is more likely to have been caused by a circulation change in the stratosphere or a change in stratosphere-troposphere dynamical coupling near the tropopause.

The corresponding temperature anomalies in the lower to middle stratosphere can be found in Figure 13. This shows the composite differences of November–January averaged temperature at 200 hPa, 50 hPa, and 10 hPa between the period 1978–1997 and the earlier and later subperiods. A common feature among the temperature anomalies at these three pressure levels is the cool anomaly over northeastern Asia. As a result, the polar stratosphere was generally colder in 1978–1997 than in the earlier and later subperiods. Note that the warm anomalies over the North Pacific are only significant in the upper troposphere (200–350 hPa); they disappear in the lower troposphere (not shown). However, as no corresponding decreases in the vertical components of EP fluxes and EP flux divergence were found in the stratosphere during 1978–1997, it is unlikely that these cooling anomalies in the polar stratosphere were induced by a reduction of planetary wave forcing from the troposphere.

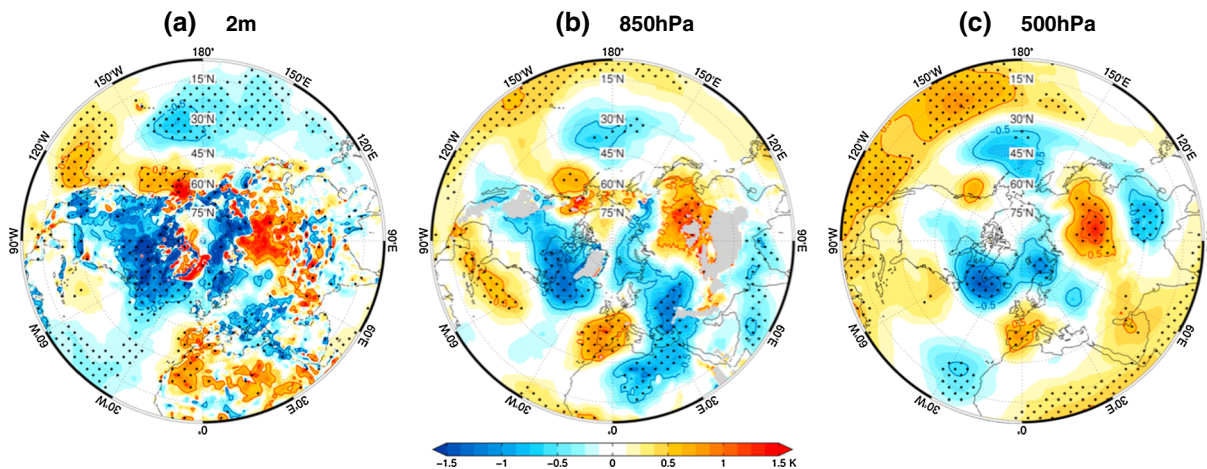


Figure 14. Same as Figure 13, but the stratospheric temperatures are replaced by (a) tropospheric temperature at 2 m above the surface, (b) 850 hPa, and (c) 500 hPa. The grey shaded areas in Figure 14b are the areas below the height of the land surface.

The composite differences of November–January mean temperatures between 1978–1997 and the earlier and later subperiods at 2 m above the surface, 850 hPa and 500 hPa, are shown in Figure 14. One dominant pattern in the temperature anomalies that is present at all the three tropospheric levels is the couplet of warm anomalies over northern Asia and cold anomalies over southern Greenland. They have the opposite sign to the temperature anomalies at 10 hPa (see Figure 13c). Another significant large-scale pattern is the couplet of positive anomalies over the subtropical North Pacific and negative temperature anomalies in the high latitudes of the North Pacific. This pattern exists mainly at 500 hPa and gets weaker at the lower levels. The anomalies resemble the Pacific–North America teleconnection pattern that is related to warm ENSO. It has been shown that ENSO affects the stratospheric polar vortex via its extratropical teleconnection with a cold ENSO leading to vortex intensification and warm ENSO leading to more SSWs [Garfinkel and Hartmann, 2008]. Because warm ENSO is linked to a warmer, more disturbed polar vortex, the warm ENSO-related temperature anomalies over the North Pacific cannot be responsible for the vortex intensification during 1978–1997. Although more detailed studies are needed to clarify the contributions from stationary, transient, and synoptic-scale Rossby waves, these tropospheric temperature anomalies also do not suggest an overall reduction of stationary planetary forcing from the troposphere during 1978–1997.

Figure 15 shows the composite differences of November–January mean sea level pressure between 1978–1997 and 1959–1976 based on ERA-40 reanalysis, between 1978–1997 and 1999–2011 based on

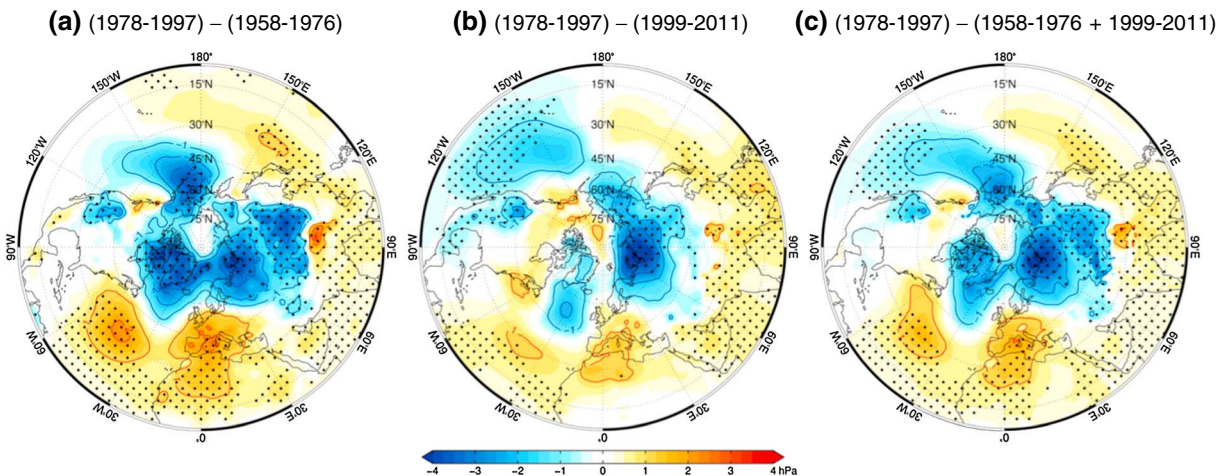


Figure 15. Polar plots of November–January mean sea level pressure composite differences of (a) 1978–1997 minus 1958–1976 based on ERA-40; (b) 1980–1997 minus 1999–2011 based on ERA-Interim; and (c) 1978–1997 minus the combined 1958–1976 and 1999–2011. The stippled areas indicate statistical significance at the $p = 0.05$ level.

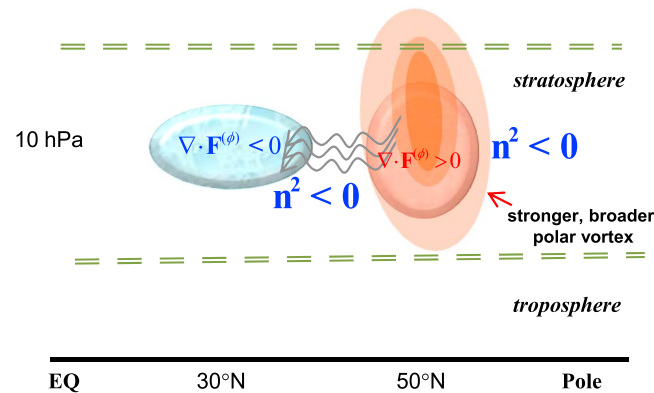


Figure 16. Schematic diagram of the anomalies of zonal mean zonal wind, EP flux divergence, and planetary wave propagation for 1978–1997. The arrows, colors, vectors, and all other symbols are the same as those in Figure 6. See text for details.

ERA-Interim, and between 1978–1997 and the earlier and later periods combined. One main feature that is common and significant in all three difference plots is the negative anomaly over the Siberian High, indicating a reduction of wave forcing from the region, but it is a region where the vertical extent of planetary waves hardly reaches into the stratosphere. The Aleutian Low and the Azores High were intensified only in the ERA-40 period, and their combined effect would lead to an enhancement of wave number 1 into the stratosphere during 1978–1997 rather than a reduction of wave forcing from the troposphere. The

intensification of the Iceland Low is also only a feature of ERA-40 periods, and the signal disappears in the ERA-Interim comparison. Thus, these results also do not support the notion that an overall reduction of planetary wave generation in the troposphere led to a significantly stronger polar vortex during 1978–1997. Thus, it is more likely that the background flow through which the waves travel has changed.

Figure 16 schematically summarizes the key process that caused the 1978–1997 disruption of the HT effect. We suggest that the mechanism proposed by Gerber and Vallis [2007] was at play. In the lower stratosphere and the upper troposphere, a broader and stronger polar vortex increased the baroclinicity of the flow at its peak axis and helped sharpen and reinforce the midlatitude jet [Robinson, 2006]. When the upward propagating synoptic waves interacted with the mean flow at the latitude of maximum winds, the divergence of wave activity generated by eddies growing within the vortex provided the momentum source for eddy-induced net acceleration of the mean flow, leading to EP flux divergence at the jet core (~40–60°N). The interaction also induced wave activity to propagate meridionally away from the jet core until it neared the critical latitudes where wave breaking occurred, indicated by the negative n^2 anomalies at 35–50°N and 65–75°N and the EP flux convergence at those latitudes (see also Figures 9 and 12). This effect on the wave driving disrupted QBO modulation of the EP fluxes at 35–50°N, 5–20 hPa, especially under eQBO. As the HT effect is most sensitive to eQBO-induced SSWs, a disruption of the wave driving under eQBO caused a weakening of the HT effect in 1978–1997.

4. Conclusions and Discussion

The temperature in the polar lower stratosphere is controlled by the radiative equilibrium temperature and the strength of the residual mean meridional circulation [Newman *et al.*, 2001]. The residual mean meridional circulation is driven by planetary-scale baroclinic wave forcing in the middle to high latitudes. The meridional and vertical propagation of planetary waves depends on the latitude-height structure of the zonal mean wind. The resulting wave guides may either reduce or enhance the number of waves getting through from the troposphere into the stratosphere.

We have studied the mechanisms behind the relationship between the QBO and the polar vortex, i.e., the Holton-Tan (HT) effect, and the cause of its weakening during 1978–1997. Based on ERA-40 and ERA-Interim reanalysis data sets over the period of 1958–2011, we find that an easterly QBO (eQBO) in the lower stratosphere leads to the formation of a midlatitude wave guide that enhances both the upward propagating planetary waves from the troposphere into the lower stratosphere (~35–50°N, 30–200 hPa) and the northward wave propagation in the upper to middle stratosphere (~35–65°N, 20–5 hPa). These EP flux anomalies induce a stronger residual mean meridional circulation in the middle to lower stratosphere and more frequent SSWs under eQBO. These results are generally in good agreement with recent studies [Naoe and Shibata, 2010; Inoue *et al.*, 2011; Yamashita *et al.*, 2011; Garfinkel *et al.*, 2012].

It is known that planetary wave propagation is sensitive to the state of the stratosphere itself [e.g., Scott and Polvani, 2004]. Modeling studies have suggested that planetary waves with intermediate amplitudes are most sensitive to QBO modulation [Holton and Austin, 1991] and that the stratospheric polar vortex becomes sensitive to the QBO near a “bifurcation” point of wave-mean flow interaction [O’Sullivan and Dunkerton, 1994]. Our results provide an additional mechanical explanation for the nonlinear behavior of the HT effect. We have found that the weakening of the HT effect in 1978–1997 was linked to a broader and stronger polar vortex. We suggest that the divergence of wave activity generated by synoptic eddies growing within the vortex provided the momentum source for wave activity to propagate meridionally away from the polar vortex, resulting in an opposite wave driving to that of the QBO, which consequently disrupted the HT effect. The weakening of the HT effect during 1978–1997 was significantly linked to the cool (warm) anomalies over northeastern Asia in the stratosphere (troposphere). Although a weak, warm ENSO teleconnection pattern was found in the near-surface temperature anomalies, this cannot be responsible for the intensification of the polar vortex during 1978–1997 as a more disturbed polar vortex would be expected under warm ENSO conditions [Garfinkel and Hartmann, 2008]. Chen and Li [2007] and Inoue and Takahashi [2013] showed that the QBO effect in the troposphere is also most significant over northeastern Asia and east Pacific region, where a cooling signal is associated with eQBO conditions. Thus, the regional signal of the QBO in the troposphere was weakened during 1978–1997 as well. Although more diagnostics are needed, our results indicate that a circulation change in the stratosphere is the main factor responsible for the weakening of the HT effect in 1978–1997.

A further result is that we have found that the differences in the seasonal mean QBO, zonal mean zonal wind, and temperature between the two ECWMF reanalysis data sets are negligibly small. There are, however, significant baseline differences in terms of the vertical EP flux component whilst the difference in the horizontal component is very small. The large difference in the vertical component of the EP fluxes and EP flux divergence between the two data sets makes it harder to differentiate the contribution due to a decadal-scale change of planetary waves in the troposphere from circulation changes in the stratosphere.

Garfinkel *et al.* [2012] suggested that the QBO-induced meridional flow forms an anomalous wave guide at $\sim 30\text{--}50^\circ\text{N}$, 5 hPa, whereby it regulates the planetary wave propagation from below. Here we have examined this mechanism in more detail using the extended ERA-reanalysis data sets. Our results fully support their mechanism. We find the change of the refractive index occurs at $\sim 35^\circ\text{N}$ and it is associated with a significant poleward wave refraction at $35\text{--}60^\circ\text{N}$, 20–5 hPa. A change of mean flow geometry caused by the QBO-induced meridional circulation at $\sim 35^\circ\text{N}$ is responsible for the change of the refractive index there. This is consistent with earlier studies that found that the critical-line mechanism is not the primary mechanism for the observed HT effect [Naoe and Shibata, 2010; Yamashita *et al.*, 2011; Garfinkel *et al.*, 2012]. However, Watson and Gray [2013] have cautioned that the critical-line mechanism is likely to be obscured by taking 3-monthly averages as in this (and previous) studies because feedbacks arising from the extratropical dynamics would modify the response at later times.

Our results may have clarified the QBO modulation of planetary waves in the lower stratosphere. Previous studies presented a mixed picture in terms of the latitudinal location as well as the seasonal variation of such modulation. Here we find that the refractive index anomalies near 60°N are opposite to those at $30\text{--}45^\circ\text{N}$ (Figure 5). This high-latitude n^2 signal is most significant in late winter but weak in early winter (not shown). As a consequence, estimating the total EP flux divergence over a large latitudinal and height extent [e.g., Dunkerton and Baldwin, 1991] or at a fixed latitude near the edge of the vortex [Ruzmaikin *et al.*, 2005; Naoe and Shibata, 2010] would lead to a weaker and/or opposite result in early and late winters. Our results show that the upward EP flux and EP flux convergence in the lower stratosphere are significantly modulated by the QBO over the extended winter period and the active latitudinal location is restricted to $\sim 35\text{--}50^\circ\text{N}$.

Previous studies have shown that the HT effect in NH winter is most significant when the QBO is defined by wind anomalies in the lower stratosphere [Naito and Yoden, 2006; Hitchman and Huesmann, 2009; Garfinkel *et al.*, 2012]. Other studies have found that equatorial forcing imposed at 10 hPa and above can also affect the polar vortex and SSWs [Gray *et al.*, 2001; Gray, 2003] and that the upper level perturbation is most noticeable in late winter [Pascoe *et al.*, 2006]. It has been suggested that the upper level QBO is the main cause of the HT effect [Naoe and Shibata, 2010; Yamashita *et al.*, 2011]. Here we find that the lower stratosphere QBO significantly alters the midlatitude wave guide, the EP fluxes, and divergence in the lower and middle

stratosphere and that the effect remains statistically significant for the extended winter period (October–March). A similar conclusion was also reached by *Inoue et al.* [2011]. The extratropical signals become much weaker when the upper stratosphere wind anomalies or wind shear are used to define the QBO (not shown). Also, the upper level QBO alone cannot explain the observed HT effect in the lower stratosphere in late October due to time needed for the upper level perturbation to be transferred downward and poleward [*Newman et al.*, 2001].

Isotta et al. [2008] found that a significant increase in synoptic wave breaking frequency in the northeastern Pacific near the tropopause occurred around the winter of 1976/1977. The warm signal in Figure 13a is consistent with the location where *Isotta et al.* [2008] detected this sudden increase in synoptic wave breaking. They attributed the anomalies to a decrease of total ozone in the extratropical lower stratosphere. Because the temperature anomalies in the stratosphere and troposphere were vertically coherent over northeastern Asia, it is plausible that a radiative change induced by stratospheric ozone depletion might have played a role in causing the vertically coherent temperature anomalies. However, more studies are needed to evaluate this. Similar to other studies [e.g., *Hu and Tung*, 2002b; *Randel et al.*, 2002], we find no evidence to support the notion that a systematic reduction of stationary planetary wave forcing from the troposphere was the responsible factor for the broadening and strengthening of the stratospheric polar vortex during 1978–1997. Thus, we suggest that a change of stratospheric circulation and/or a change of the stratosphere-troposphere coupling were the main causes for the disrupted HT effect in 1978–1997. Further studies are needed to clarify what caused the broadening of the lower stratospheric polar vortex during the period and whether or not the decadal-scale variation of the upward wave forcing from the troposphere also played a role.

Acknowledgments

H.L., T.J.B., and T.P. were supported by the UK Natural Environment Research Council (NERC). This study is part of the British Antarctic Survey Polar Science for Planet Earth Programme. We acknowledge use of ECMWF reanalysis data sets. L.J.G. is also supported by NERC, through the National Centre for Atmospheric Science (NCAS). We thank the three anonymous reviewers for their constructive comments.

References

- Andrews, D. G., J. R. Holton, and C. B. Leovy (1987), *Middle Atmosphere Dynamics*, Academic Press INC. LTD, London.
- Anstey, J. A., and T. G. Shepherd (2008), Response of the northern stratospheric polar vortex to the seasonal alignment of QBO phase transitions, *Geophys. Res. Lett.*, *35*, L22810, doi:10.1029/22008GL035721.
- Anstey, J. A., and T. G. Shepherd (2013), High-latitude influence of the quasi-biennial oscillation, *Q. J. R. Meteorol. Soc.*, doi:10.1002/qj.2132.
- Balachandran, N. K., and D. Rind (1995), Modeling the effects of UV variability and the QBO on the troposphere-stratosphere system. Part I: The middle atmosphere, *J. Clim.*, *8*, 2058–2079.
- Baldwin, M. P., et al. (2001), The quasi-biennial oscillation, *Rev. Geophys.*, *39*(2), 179–229.
- Calvo, N., M. A. Giorgetta, R. Garcia-Herrera, and E. Manzini (2009), Nonlinearity of the combined warm ENSO and QBO effects on the Northern Hemisphere polar vortex in MAECHAM5 simulations, *J. Geophys. Res.*, *114*, D13109, doi:10.1029/2008JD011445.
- Camp, C. D., and K. K. Tung (2007), The influence of the solar cycle and QBO on the late-winter stratospheric polar vortex, *J. Atmos. Sci.*, *64*, 1267–1283.
- Chen, W., and T. Li (2007), Modulation of northern hemisphere wintertime stationary planetary wave activity: East Asian climate relationships by the Quasi-Biennial Oscillation, *J. Geophys. Res.*, *112*, D20120, doi:10.1029/22007JD008611.
- Dee, D. P., and S. Uppala (2009), Variational bias correction of satellite radiance data in the ERA-Interim reanalysis, *Quart. J. R. Meteorol. Soc.*, *135*, 1830–1841.
- Dunkerton, T. J., and M. P. Baldwin (1991), Quasi-biennial modulation of planetary wave fluxes in the Northern Hemisphere winter, *J. Atmos. Sci.*, *48*, 1043–1061.
- Garfinkel, C. I., and D. L. Hartmann (2008), Different ENSO teleconnections and their effects on the stratospheric polar vortex, *J. Geophys. Res.*, *113*, D18114, doi:10.1029/2008JD009920.
- Garfinkel, C. I., T. A. Shaw, D. L. Hartmann, and D. W. Waugh (2012), Does the Holton–Tan mechanism explain how the quasi-biennial oscillation modulates the Arctic polar vortex?, *J. Atmos. Sci.*, *69*, 1713–1733.
- Gerber, E. P., and G. K. Vallis (2007), Eddy–zonal flow interactions and the persistence of the zonal index, *J. Atmos. Sci.*, *64*, 3296–3311, doi:10.1175/JAS4006.1.
- Gray, L. J. (2003), The influence of the equatorial upper stratosphere on stratospheric sudden warmings, *Geophys. Res. Lett.*, *30*(4), 1166, doi:10.1029/2002GL016430.
- Gray, L. J., and J. A. Pyle (1989), A two-dimensional model of the quasi-biennial oscillation of ozone, *J. Atmos. Sci.*, *46*, 203–220, doi:10.1175/1520-0469(1989)046<0203:ATDMOT>2.0.CO;2.
- Gray, L. J., S. J. Phipps, T. J. Dunkerton, M. P. Baldwin, E. F. Drysdale, and M. R. Allen (2001), A data study of the influence of the equatorial upper stratosphere on northern-hemisphere stratospheric sudden warmings, *Q. J. R. Meteorol. Soc.*, *127*(576), 1985–2003.
- Hamilton, K. (1998), Effects of an imposed quasi biennial oscillation in a comprehensive troposphere stratosphere mesosphere general circulation model, *J. Atmos. Sci.*, *55*, 2393–2418.
- Haynes, P. H., C. J. Marks, M. E. McIntyre, T. G. Shepherd, and K. P. Shine (1991), On the “downward control” of extratropical diabatic circulations by eddy-induced mean zonal forces, *J. Atmos. Sci.*, *48*, 651–678.
- Hitchman, M. H., and A. S. Huesmann (2009), Seasonal influence of the quasi-biennial oscillation on stratospheric jets and Rossby wave breaking, *J. Atmos. Sci.*, *66*, 935–946.
- Holton, J. R., and J. Austin (1991), The influence of the equatorial QBO on sudden stratospheric warmings, *J. Atmos. Sci.*, *48*, 607–618.
- Holton, J. R., and H. C. Tan (1980), The influence of the equatorial quasi-biennial oscillation on the global circulation at 50 mb, *J. Atmos. Sci.*, *37*, 2200–2208.
- Holton, J. R., and H. C. Tan (1982), The quasi-biennial oscillation in the Northern Hemisphere lower stratosphere, *J. Meteor. Soc. Japan*, *60*, 140–148.

- Hu, Y., and K. K. Tung (2002a), Tropospheric and equatorial influences on planetary-wave amplitude in the stratosphere, *Geophys. Res. Lett.*, *29*(21019), doi:10.1029/2001GL013762.
- Hu, Y., and K. K. Tung (2002b), Interannual and decadal variations of planetary wave activity, stratospheric cooling, and Northern Hemisphere annular mode, *J. Clim.*, *15*, 1659–1673.
- Inoue, M., and M. Takahashi (2013), Connections between the stratospheric quasi-biennial oscillation (QBO) and tropospheric circulation over Asia in Northern autumn, *J. Geophys. Res. Atmos.*, *118*, 10,740–10,753, doi:10.1002/jgrd.50827.
- Inoue, M., M. Takahashi, and H. Naoe (2011), Relationship between the stratospheric quasi-biennial oscillation (QBO) and tropospheric circulation in northern autumn, *J. Geophys. Res.*, *116*, D24115, doi:10.1029/2011JD016040.
- Isotta, F., O. Martius, M. Sprenger, and C. Schwierz (2008), Long-term trends of synoptic-scale breaking Rossby waves in the Northern Hemisphere between 1958 and 2001, *Int. J. Climatol.*, *28*, 1551–1562, doi:10.1002/joc.1647.
- Killworth, P. D., and M. E. McIntyre (1985), Do Rossby-wave critical layers absorb, reflect, or over-reflect?, *J. Fluid Mech.*, *161*, 449–492.
- Kinnersley, J. S., and K. K. Tung (1998), Modeling the global interannual variability of ozone due to the equatorial QBO and to extratropical planetary wave variability, *J. Atmos. Sci.*, *55*, 1417–1428, doi:10.1175/1520-0469(1998)055<1417:MTGIVO>2.0.CO;2.
- Kodera, K. (1991), The solar and equatorial QBO influences on the stratospheric circulation during the early northern-hemisphere winter, *Geophys. Res. Lett.*, *18*, 1023–1026.
- Labitzke, K., and H. van Loon (1988), Associations between the 11-year solar-cycle, the QBO and the atmosphere 1. The troposphere and stratosphere in the Northern Hemisphere in winter, *J. Atmos. Sol. Terr. Phys.*, *50*(3), 197–206.
- Lu, H., M. P. Baldwin, L. J. Gray, and M. J. Jarvis (2008), Decadal-scale changes in the effect of the QBO on the northern stratospheric polar vortex, *J. Geophys. Res.*, *113*, D10114, doi:10.1029/2007JD009647.
- Lu, H., L. J. Gray, M. P. Baldwin, and M. J. Jarvis (2009), Life cycle of the QBO-modulated 11-year solar cycle signals in the Northern Hemispheric winter, *Q. J. R. Meteorol. Soc.*, *135*, 1030–1043.
- Marshall, A. G., and A. A. Scaife (2009), Impact of the QBO on surface winter climate, *J. Geophys. Res.*, *114*, D18110, doi:10.1029/2009JD011737.
- Naito, Y., and I. Hirota (1997), Interannual variability of the northern winter stratospheric circulation related to the QBO and the solar cycle, *J. Met. Soc. Japan*, *75*, 925–937.
- Naito, Y., and S. Yoden (2006), Behavior of planetary waves before and after Stratospheric Sudden Warming events in several phases of the equatorial QBO, *J. Atmos. Sci.*, *63*, 1637–1649.
- Naoe, H., and K. Shibata (2010), Equatorial quasi-biennial oscillation influence on northern winter extratropical circulation, *J. Geophys. Res.*, *115*, D19102, doi:10.1029/2009JD012952.
- Newman, P. A., E. R. Nash, and J. E. Rosenfield (2001), What controls the temperature of the Arctic stratosphere during the spring?, *J. Geophys. Res.*, *106*, 19,999–20,010, doi:10.1029/2000JD000061.
- O'Sullivan, D., and T. J. Dunkerton (1994), Seasonal development of the extratropical QBO in a numerical model of the middle atmosphere, *J. Atmos. Sci.*, *51*, 3706–3722.
- O'Sullivan, D., and M. Salby (1990), Coupling of the quasi-biennial oscillation and the extratropical circulation in the stratosphere through planetary wave transport, *J. Atmos. Sci.*, *47*, 650–673.
- O'Sullivan, D., and R. E. Young (1992), Modeling the quasi-biennial oscillation's effect on the winter stratospheric circulation, *J. Atmos. Sci.*, *49*, 2437–2448.
- Pascoe, C. L., L. J. Gray, and A. A. Scaife (2006), A GCM study of the influence of equatorial winds on the timing of sudden stratospheric warmings, *Geophys. Res. Lett.*, *33*, L06825, doi:10.1029/2005GL024715.
- Plumb, R. A., and R. C. Bell (1982), A model of the quasi-biennial oscillation on an equatorial beta-plane, *Q. J. R. Meteorol. Soc.*, *108*, 335–352.
- Randel, W. J., F. Wu, and R. Stolarski (2002), Changes in column ozone correlated with the stratospheric EP flux, *J. Meteor. Soc. Japan*, *80*, 849–862.
- Robinson, W. A. (2006), On the self-maintenance of midlatitude jets, *J. Atmos. Sci.*, *63*, 2109–2122.
- Ruzmaikin, A., J. Feynman, X. Jiang, and Y. L. Yung (2005), Extratropical signature of the quasi-biennial oscillation, *J. Geophys. Res.*, *110*, D11111, doi:10.1029/2004JD005382.
- Scott, R. K., and L. M. Polvani (2004), Stratospheric control of upward wave flux near the tropopause, *Geophys. Res. Lett.*, *31*, L02115, doi:10.1029/2003GL017965.
- Tung, K. K. (1979), A theory of stationary long waves. Part III: Quasi-normal modes in a singular waveguide, *Mon. Weather Rev.*, *107*, 751–774, doi:10.1175/1520-0493(1979)107<0751:ATOSLW>2.0.CO;2.
- Uppala, S. M., et al. (2005), The ERA-40 reanalysis, *Q. J. R. Meteorol. Soc.*, *131*(612), 2961–3012.
- Watson, P. A. G., and L. J. Gray (2013), How does the quasi-biennial oscillation affect the stratospheric polar vortex?, *J. Atmos. Sci.*, *71*, 391–409, doi:10.1175/JAS-D-13-096.1.
- Wei, K., W. Chen, and R. Huang (2007), Association of tropical Pacific sea surface temperatures with the stratospheric Holton-Tan oscillation in the Northern Hemisphere winter, *Geophys. Res. Lett.*, *34*, L16814, doi:10.1029/2007GL030478.
- Yamashita, Y., H. Akiyoshi, and M. Takahashi (2011), Dynamical response in the Northern Hemisphere midlatitude and high-latitude winter to the QBO simulated by CCSR/NIES CCM, *J. Geophys. Res.*, *116*, D06118, doi:10.1029/2010JD015016.